

# Effect of the spanwise grid spacing and treatment of convection term in DES

Chi-Su Song\* and Seung-O Park\*

Department of Aerospace Engineering, KAIST, Daejeon, KOREA

## Abstract

A two-dimensional backward facing step flow was computed using a Detached Eddy simulation (DES) based on the SST turbulence model. The expansion ratio (ER) was 1.125 and the Reynolds number based on the step height and the mean velocity in the upstream channel was 37,500. The flow condition was the same as with the experimental research [1]. The reattachment length, oscillatory characteristics of the flow and the coherent structures of the present simulation were compared to demonstrate the importance of spanwise grid spacing.

**Key Word :** Two-dimensional backward facing step flow, Hybrid RANS/LES, Detached Eddy Simulation, Spanwise grid spacing

## Introduction

Several simulation methods known as hybrid RANS/LES, such as DES, VLES (Very Large Eddy Simulation) [2] and PANS (Partially Averaged Navier-Stokes) [3] have been proposed. These methods are proposed to efficiently combine the advantages of RANS (Reynolds Averaged Navier-Stokes) and LES (Large Eddy Simulation). The DES method, which simulates massively separated flows [4-5], was chosen in this work. The most widely used baseline turbulence models of DES are the S-A (Spalart-Allmaras) model [6] and the SST (Shear Stress Transport) model [7].

Several versions of DES and URANS were applied in our previous study [8] to simulate a two-dimensional backward facing step (BFS) flow with the grid system suggested in NPARC alliance [9]. The solution was converged to steady state in the case of URANS simulation, indicating that the URANS approach was not suitable in simulating unsteady phenomena of BFS flow. Four cases in DES simulation were tested to investigate the effect of numerical scheme for the convective term in the Navier-Stokes equation. The applied numerical schemes were the 5<sup>th</sup> order upwind scheme and a hybrid scheme combining the upwind and the central scheme [10]. The effect of treatment of convective term was negligible in DES based on S-A model. The difference between the case of upwind scheme and that of hybrid scheme was significant in DES based on SST model, especially for the frequency characteristics of unsteady motion and coherent structures.

The effect of spanwise grid spacing on simulation results was investigated in the present work. The sensitivity of length scale formulation and grid spacing on the simulation using DES has been studied [11]. The spanwise grid spacing is usually taken to be much coarser than the spacing in the other two directions (streamwise and wall normal directions)

---

\* Professor, Aerospace Engineering Dept, KAIST

E-mail : [sopark@kaist.ac.kr](mailto:sopark@kaist.ac.kr)

Tel : 82-42-869-3785

Fax : 82-42-869-3750

The length scale for DES with this practice is likely to be governed by spanwise grid spacing. The effect of spanwise grid spacing in DES based on SST turbulence model employing two different discretization schemes, namely the upwind scheme and the hybrid scheme. Results of the present DES were compared with those of LES [12] and experiment [1].

## Numerical Method

The three dimensional incompressible Navier–Stokes equations were integrated using a fully implicit fractional step method. The governing equations were transformed to generalized curvilinear coordinates on a non–staggered grid. Time integration was done using a double time stepping algorithm and local time stepping was used to accelerate the convergence. All terms except for the convective term in the momentum and pressure–Poisson equations were approximated using the second–order central difference scheme.

### 2.1 SST based DES formulation

DES formulation [5], which is based on a SST turbulence model, was used. The length scale representative of turbulent transport in the original SST turbulence model is given by:

$$l_{turb} = k^{\frac{1}{2}} / (\beta^* \omega). \quad (1)$$

The DES formulation of SST model was obtained by redefining the length scale in the dissipative term of the transport equation for the modeled turbulent kinetic energy as follows [7]:

$$l_{DES} = \min(l_{turb}, C_{DES} \Delta) \quad (2)$$

Eq. (2) implies that away from solid boundaries the turbulence length scale of DES is proportional to the local grid size,  $\Delta$  as in LES.  $\Delta$  is defined by:

$$\Delta = \max(\Delta x, \Delta y, \Delta z). \quad (3)$$

The model parameter  $C_{DES}$  was obtained from Eq. (4) using the blending function  $F_1$  proposed by Menter [4]:

$$C_{DES} = (1 - F_1) C_{DES}^{k-\varepsilon} + F_1 C_{DES}^{k-\omega} \quad (4)$$

where  $F_1 = \tanh \left\{ \left( \min \left[ \max \left[ \frac{\sqrt{k}}{0.09 \omega y}, \frac{500 \mu}{\rho y^2 \omega} \right], \frac{4 \rho \sigma_{\omega 2} k}{CD_{k\omega} y^2} \right] \right)^4 \right\}$ ,

$$CD_{k\omega} = \max \left[ \frac{2 \rho \sigma_{\omega 2}}{\omega} \frac{\partial k}{\partial x_j} \frac{\partial \omega}{\partial x_j}; 10^{-20} \right] \quad C_{DES}^{k-\varepsilon} = 0.61, \quad C_{DES}^{k-\omega} = 0.78, \quad \sigma_{\omega 2} = 0.856.$$

With the above arrangements, the eddy viscosity,  $\nu_t$ , was evaluated in the same manner as in the conventional SST model as follows:

$$\nu_t = \frac{k / \omega}{\max \left[ 1; \Omega F_2 / (a_1 \omega) \right]} \quad (5)$$

where  $a_1 = 0.31$ ,  $F_2 = \tanh \left\{ \left( \max \left[ 2 \frac{\sqrt{k}}{0.09\omega y}; \frac{500\mu}{\rho y^2 \omega} \right] \right)^2 \right\}$  with  $y$  being the normal distance from the wall.

## 2.2 Numerical scheme for convective term

Two kinds of differencing schemes for the convective term were employed. The convective term was discretized either by using the 5<sup>th</sup> order upwind scheme or by using the hybrid scheme (5<sup>th</sup> upwind/2<sup>nd</sup> central scheme) which was developed to minimize the level of numerical dissipation away from solid boundaries [10]. The blending function  $\sigma$  for switching upwind/central scheme is given by:

$$\sigma = \sigma_{\max} \tanh(A^{C_{H1}}). \quad (6)$$

Here the function A is defined as:

$$A = C_{H2} \max \left\{ \left[ (C_{DES} \Delta / l_{turb}) / g - 0.5 \right], 0 \right\} \quad (7)$$

where  $l_{turb}$  is the length scale from turbulence model and  $g = \tanh B^4$ .

The other coefficients in the above equations are:

$$B = C_{H3} \Omega \max(S, \Omega) / \max \left[ (S^2 + \Omega^2) / 2, 10^{-20} \right], \quad \sigma_{\max} = 1.0, \quad C_{H1} = 3.0, \\ C_{H2} = 1.0, \quad C_{H3} = 2.0.$$

The hybrid differencing is then formulated as:

$$F_{inv} = (1 - \sigma) F_{central} + \sigma F_{upwind} \quad (8)$$

where  $F$  denotes the inviscid flux.

## COMPUTATIONAL DETAILS

### 3.1 Computational domain and grids

A two-dimensional BFS flow with the expansion ratio (ER) of 1.125 was chosen as a target flow. The Reynolds number, defined with the step height (H) and the mean velocity in the upstream channel, was 37,500, a corresponding condition with experiment [1]. A sketch of the computational domain is provided in Fig. 1. The length of the computational domain in the spanwise direction was 2H. The periodic condition was employed in this direction. The non-dimensional time step, defined by  $tU/H$ , of 0.05 for the present simulation was used, which is sufficient value to track the unsteady characteristics of BFS flow. The basic grid system, streamwise and wall normal direction (Fig. 2) suggested by NPARC alliance [9], was used in all simulation cases:  $\Delta x_{\min}^+ = 1.75$ ,  $\Delta z_{\min}^+ = 1.29$ ,  $N_x = 163$ , and  $N_z = 185$ . The friction velocity to estimate the wall coordinates was taken at the right control volume of the entrance region near the corner of the step. Grid spacing in the spanwise direction was changed with the grid system fixed in the X-Z plane. The spanwise grid spacing was often greater than wall normal and streamwise grid spacing. The length scale of DES in this case was dominantly determined by spanwise grid spacing (Eq. 3). Thus, the variation of spanwise grid spacing amounts to the change of the length scale for DES. The grid spacing

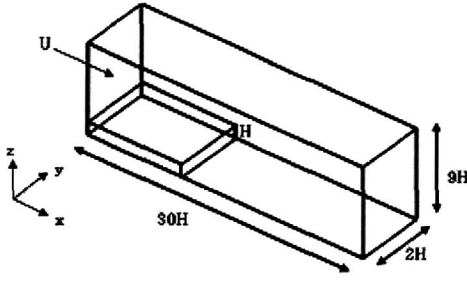


Fig. 1. Computational domain

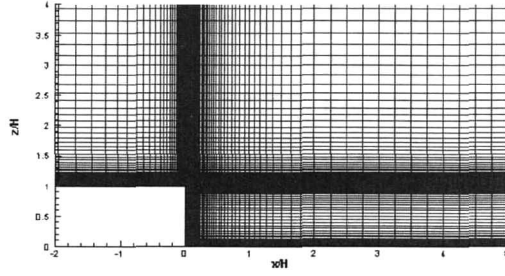


Fig. 2. Basic grid system in X-Z plane

used in the present work is given in Table 1. The spanwise grid spacing,  $\Delta y^+ = 24.5$ , was used in LES of BFS flow ( $ER=1.2$  &  $Re_H=28,000$ ) [13]. The present spanwise grid was much coarser than for the LES grid [13] (Table 1).

### 3.2 Effect of spanwise grid spacing

The normalized turbulent length scale ( $l_{turb}/H$ ) was evaluated from the URANS simulation results. The normalized turbulent length scale in the separation–reattachment–redeveloping (SRR) region beyond the step was much greater than its value in the channel center region (Fig. 3).  $C_{DES}\Delta$  in this SRR region was much smaller than  $l_{turb}$ , and hence was selected as  $l_{DES}$  (Eq. (2)).

Table 1. Grid information for spanwise direction

	Grid resolution & Number of grids on spanwise direction		
	$\Delta y^+ = 142$ $N_y = 24$ $\Delta y = 0.0833$	$\Delta y^+ = 95$ $N_y = 36$ $\Delta y = 0.0555$	$\Delta y^+ = 71$ $N_y = 48$ $\Delta y = 0.0416$
Simulation cases	SST DES–Upwind 24	SST DES–Upwind 36	SST DES–Upwind 48
	SST DES–Hybrid 24	SST DES–Hybrid 36	SST DES–Hybrid 48

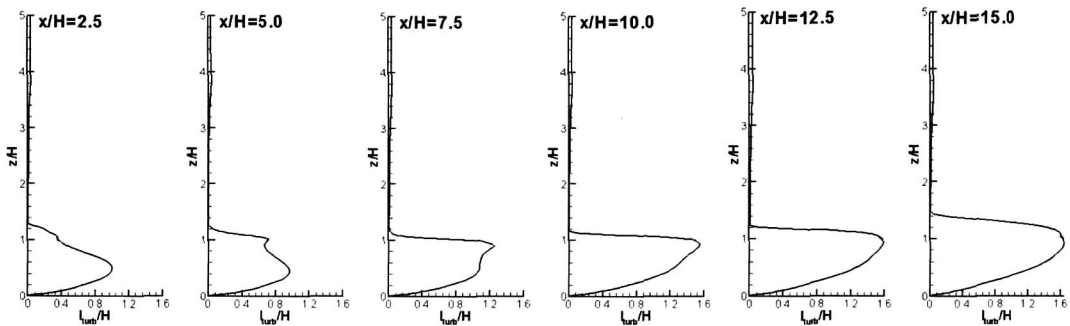
Fig. 3. Normalized turbulent length scale ( $l_{turb}/H$ )

Table 2. Range of  $\Delta$ 

Number of spanwise grid	Range of $\Delta$ from Eq. (3)
$N_y = 24$	$0.0833 < \Delta < 0.95$
$N_y = 36$	$0.0555 < \Delta < 0.95$
$N_y = 48$	$0.0416 < \Delta < 0.95$

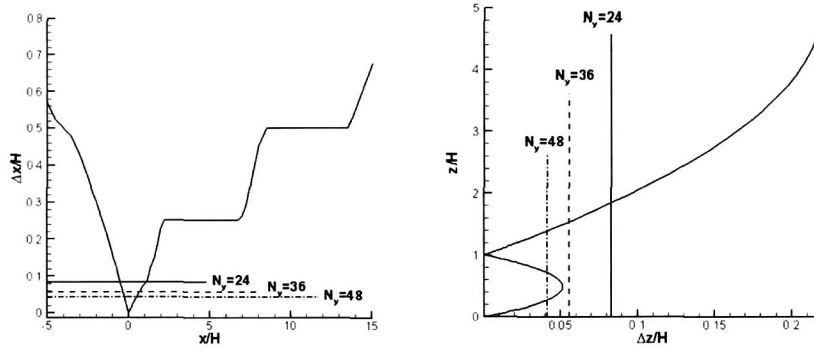
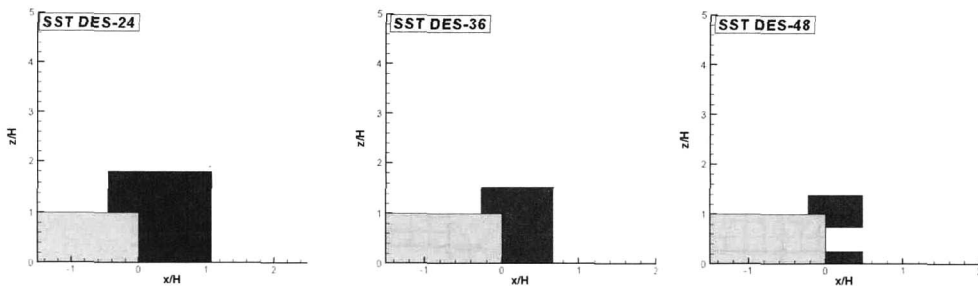


Fig. 4. Normalized grid spacing of streamwise and wall normal direction with the number of spanwise direction grid

The range of  $\Delta$  values in the three different simulation cases is shown in Table 2. The maximum  $\Delta$  was the same in all the three cases as determined by  $\Delta x$  (which was fixed in all the cases). However, minimum  $\Delta$  was different as determined by the spanwise grid spacing. The grid spacing distributions in the streamwise ( $\Delta x$ ) and the wall normal ( $\Delta z$ ) directions in comparison with the spanwise grid spacing is shown in Fig. 4.

The streamwise and wall normal direction grids were finely constructed in the near wall region around the step (Fig. 4). Thus, spanwise direction grid spacing ( $\Delta y$ ) was dominantly selected as  $\Delta$  (Eq. 3). The region where  $\Delta$  was determined by the spanwise grid spacing,  $\Delta y$ , is shown in Fig. 5. The region, where  $\Delta$  was equal to  $\Delta y$ , is reduced as  $\Delta y$  became smaller (Fig. 5).

The region where the length scale ( $l_{turb}$ ) from the turbulence model was selected by the DES calculation is shown in Fig. 6. The view was enlarged for the wall region adjacent to the step. The region of  $l_{turb}$  became smaller as the spanwise grid spacing becomes smaller (Eq. 2).

Fig. 5. Region where  $\Delta$  determined by spanwise grid spacing

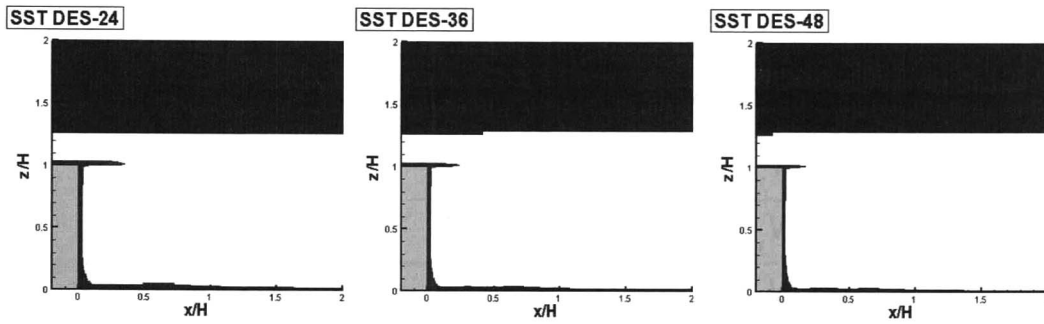


Fig. 6. Region where RANS is simulated (enlarged view)

## Results

### 4.1 Skin friction distribution and reattachment length

Skin friction along the bottom wall is shown in Fig. 7. The predicted reattachment lengths with the differences between our results and the experimental result [1] are given in Table 3. Skin friction distribution curves from the simulation were in good agreement with experimental data [1], except for the case of SST DES–Upwind 24 (Fig. 7). The reattachment length and skin friction distribution became closer to experimental data [1] as the spanwise grid became denser for the cases of the upwind scheme. In contrast, simulation with the hybrid scheme was insensitive to spanwise grid spacing (Fig. 7).

Table 3. Reattachment length and difference with experimental data [1]

Simulation cases	Reattachment length (x/H)	Difference with exp. (%)
SST DES – Upwind 24	7.00	+11.80
SST DES – Upwind 36	6.55	+4.65
SST DES – Upwind 48	6.42	+2.55
SST DES – Hybrid 24	6.45	+3.03
SST DES – Hybrid 36	6.42	+2.55
SST DES – Hybrid 48	6.40	+2.23
Exp. [1]	6.26	/

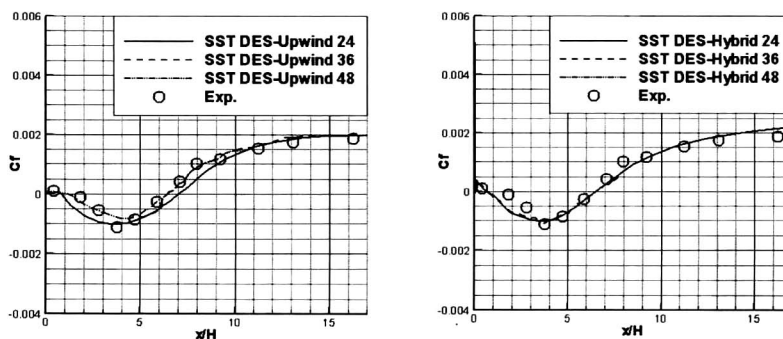


Fig. 7. Skin friction distribution

## 4.2 Frequency of shear layer oscillation

BFS flow is unstable due to separation at the edge of the step [12]. Time-histories of streamwise velocity fluctuation at  $x/H=6$  and  $z/H=1$  in present numerical simulation and experimental data [14], which was measured by a hot wire system, are shown in Fig. 8. The monitoring station was at  $x/H=6.5$  and  $z/H=1$  in cases of SST URANS, SST DES-Upwind 24 and SST DES-Hybrid 24.

Solutions converged to steady state and failed to simulate unsteady characteristics of the flow in the case of URANS. On the contrary, the velocity signal clearly showed oscillatory features in all SST-DES simulations whereas the SST DES-upwind24 case exhibited much smaller amplitude fluctuation than the other cases. Not only the discretization scheme, but also the spanwise grid spacing, strongly influenced the behavior of velocity fluctuation (Fig. 8).

The flow oscillated with the Strouhal number ( $fH/U$ ) of the dominant peak of 0.096 in Driver et al.'s experiment [14]. The frequency from the LES study [12] was 0.08 ( $ER=1.6$  and  $Re_H=38,000$ ). The dominant frequencies of the present simulation obtained from the vertical velocity fluctuations are summarized in Table 4 and Fig. 9. The frequencies and spectrums obtained with the upwind scheme widely varied with the spanwise grid spacing. This signified that the simulation with the upwind scheme required far more rigorous grid independence test than the hybrid scheme. The predictions with the hybrid scheme were much less sensitive to the grid spacing (Table 4 and Fig. 9).

Table 4. Comparison of non-dimensional strouhal number

	SST DES-Upwind		SST DES-Hybrid	
	DES	Upwind-24	0.170, 0.240	Hybrid-24
	Upwind-36	0.086, 0.152	Hybrid-36	0.045, 0.090, 0.15
	Upwind-48	0.091, 0.260	Hybrid-48	0.046, 0.092
Experiment[14]	0.096			
LES[12]	0.080			

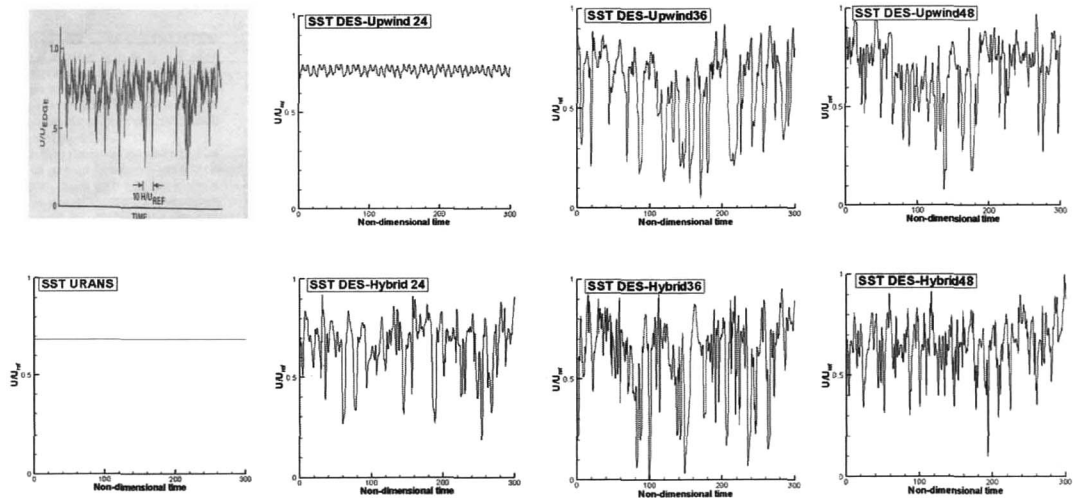


Fig. 8. Time history of streamwise velocity fluctuation

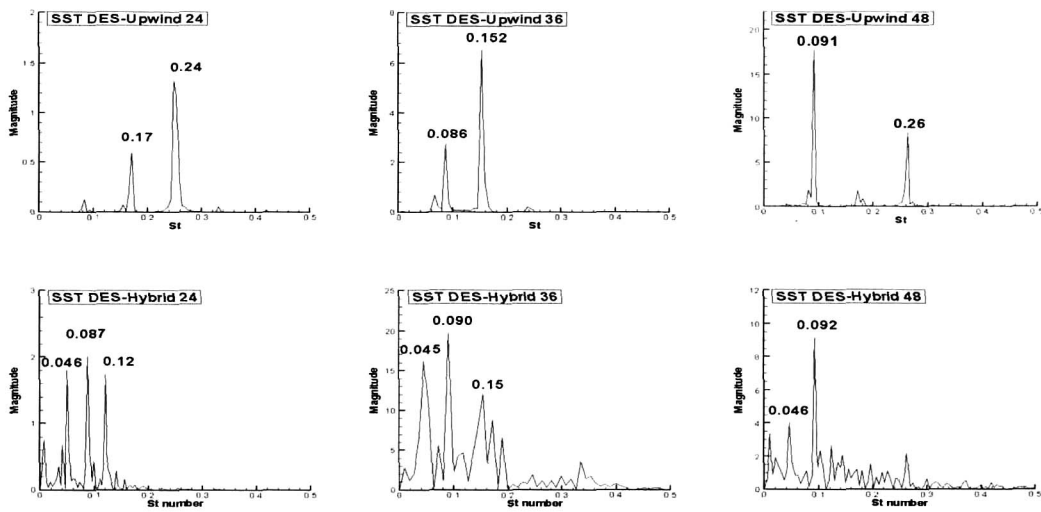


Fig. 9. Dominant frequency of BFS on S-A DES and SST DES-hybrid

### 4.3 Vortical structure

Vortices are stretched in the shear layer beyond the step, as in the mixing layer. These large scale structures persist for an appreciable distance downstream. Instantaneous vorticity contours of some cases in the present simulation, LES result [12] are presented in Fig. 10. The solutions converged to steady state, and thus, the vortical structure was nearly fixed with time in the URANS case. The present simulations, except for the case of SST DES-upwind 24, produced very similar vorticity contours to that of LES.

$Q$  criterion proposed by Hunt et al. [15] was adopted to clearly identify the vortical structures. The  $Q$ -criterion defines the regions where the second invariant of velocity gradient tensor  $Q$  is positive as vortex tubes. The quantity  $Q$  is defined by:

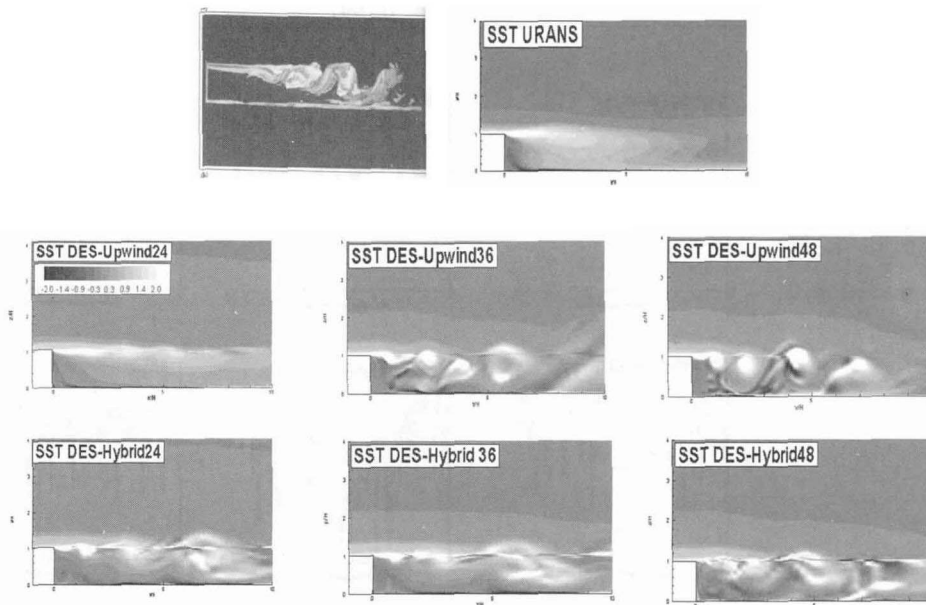


Fig. 10. Instantaneous vorticity contour



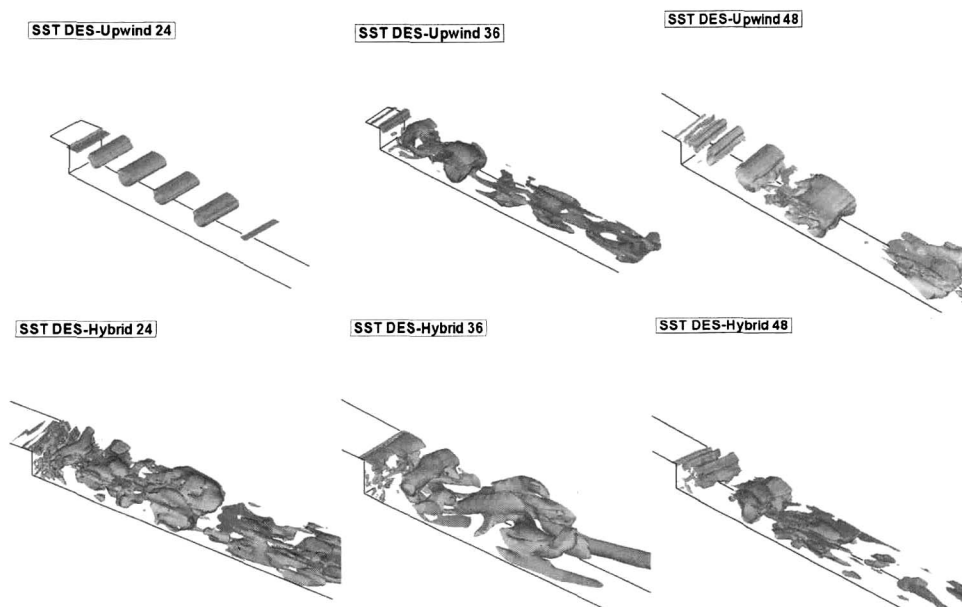


Fig. 11. Q criterion coherent structure

## Conclusion

The importance of numerical scheme for convection term and spanwise grid spacing in DES based on the SST turbulence model was investigated for a two-dimensional backward facing step flow.

When the spanwise grid system was coarse, the results of mean quantities, such as the skin friction and the reattachment length for the case of DES with the upwind scheme, were poorly predicted compared to the other simulations. Prediction of mean quantities was improved as the number of spanwise grid was increased. On the other hand, DES with hybrid scheme produced similar results for the mean quantities for all three different spanwise grid spacing cases. This suggested that the grid independence test for the upwind scheme should be carried out very carefully.

The dominant oscillation frequency of DES cases with upwind scheme depended significantly on spanwise grid spacing. The frequency content of velocity fluctuation largely deviated from the experimental data except for SST DES-Upwind 48 case. On the contrary, DES cases with the hybrid scheme were insensitive to spanwise grid spacing in predicting both mean and fluctuating quantities, other than the details of the coherent structures.

## Acknowledgment

This research was supported by Underwater Vehicle Research Center at Korea Maritime University under the sponsorship of Ministry of National Defense and Agency for Defense Development.

## References

1. Driver, D. M. and Seegmiller, H. L., Features of a Reattaching Turbulent Shear Layer in Divergent Channel Flow, *AIAA Journal*, Vol. 23, No. 2 pp. 163–171, 1985.
2. Speziale, C.G., Turbulence modelling for time-dependent RANS and VLES: a review *AIAA Journal*, Vol. 38, No. 2 pp. 173–183, 1998.

3. Girimaji, S. S., Partially Averaged Navier–Stokes model for turbulence: A Reynolds–Averaged Navier–Stokes to direct numerical simulation bridging method, *Journal of Applied Mechanics*, Vol. 73, pp. 413–421, 2006.
4. Spalart, P. R., Jou, W. H., Strelets, M., and Allmaras, S. R., Comments on the feasibility of LES for wings and on a hybrid RANS/LES approach, *Advances in DNS /LES: First AFOSR Int. Conf. on DNS/LES*, Greyden, Columbus, 1997.
5. Strelets, M., Detached Eddy Simulation of massively Separation Flows, AIAA paper, 2001–0879, 2001.
6. Spalart, P. R. and Allmaras, S. R., A one equation turbulence model for aerodynamics flows, AIAA paper, 1992–0439, 1992.
7. Menter, P. R., Zonal two–equation  $k-\omega$  turbulence models for aerodynamic flows, AIAA paper, 1993–2906, 1993.
8. Song, C. S. and Park, S. O., Assessment of URANS and DES for two–dimensional backward facing step flow, *JSASS–KSAS Joint International Symposium on Aerospace Engineering*, Nagoya, Japan, Oct, 2005.
9. NPARC Alliance CFD Verification and Validation Web Site  
(<http://www.grc.nasa.gov/WWW/wind/valid/validation.htm>)
10. Travin, A., Shur, M., Strelets, M., and Spalart, P. R., Physical and numerical upgrades in the detached–eddy simulation of complex turbulent flows, In: 412 *EUROMECH Colloquium on LES of Complex transitional and turbulent flows*, Munich, Oct. 2000.
11. Yan, J., Mockett, C., and Thiele, F., Investigation of alternative length scale substitutions in Detached Eddy Simulation, *Flow, Turbulence and combustion*, Vol. 74, pp. 85–102, 2005.
12. Neto, A. S., Grans, D., Metais, O and Lesieur, M., A numerical investigation of the coherent vortices in turbulence behind a backward facing step, *Journal of Fluid Mechanics*, Vol. 256, pp. 1–25, 1993.
13. Akselvoll, K. and Moin, P., Large eddy simulation of turbulent confined coannular jets and turbulent flow over a backward facing step, Report No. TF–63, Stanford University, 1995
14. Driver, D. M., Seegmiller, H. L. and Marvin J. G., Time–Dependent Behavior of a Reattaching Shear Layer, *AIAA Journal*, Vol. 25, No. 7 pp. 914–919, 1987.
15. Hunt, J. C. R., Wrat, A. A., and Moin, P., Eddies, stream, and convergence zones in turbulent flows, in *Proceedings of the 1988 Summer Program (CTR, Stanford, CA, 1988)*, pp. 193–208, 1988.